UV Light Detection by Sno$_2$-Rgo Nanohybrid Based Sensing Platform

Sonal Rattan[1,2*],Twinkle Pal[3], Anjali Leal[4],Suresh Kumar[4], J.K.Goswamy[4]

[1]Department of UCRD, Chandigarh University, Gharuan, Mohali, Punjab, India, 140413

[2]AIT (CSE), Chandigarh University, Gharuan, Mohali, Punjab, India, 140413

[3] Department of Physics, Rayat and Bahara University, Mohali, Punjab, India, 140104

[4]Department of Applied Sciences, UIET, Panjab University, Chandigarh, India

[*]Corresponding Author E-mail: _sonalrattan.zenith@gmail.com_

ABSTRACT

In present study a facile single step methodology for synthesising SnO$_2$-rGO nanohybrid by extracting metal ions from the tin chloride precursor, leading to the formation of SnO$_2$ nanoparticles is reported. The structure formed via this method was characterized using X-ray diffractometry (XRD), UV-visible spectroscopy, Fourier transformed infrared (FTIR) spectroscopy, field emission scanning electron microscopy (FESEM) and Energy dispersive X-ray spectroscopy (EDS) .Surface morphology displayed the SnO$_2$ nanoparticles densely loaded in between the graphene sheets. The nanohybrid was found responsive towards the incident UV light. This approach can lead to the development of flexible light detectors having quick response.

Keywords: Nanohybrid, Diffractometry, Morphology.

1. INTRODUCTION

Semiconductor photodetectors use the capabilities of nanomaterials to transform incoming light having a certain wavelength into a detectable electrical output (photocurrent). Hybridization of nanoparticles with advanced 2D materials like graphene is an interesting methodology, which has been employed for enhanced photodetection applications. Graphene possesses excellent optoelectronic attributes because of its distinct electronic band structure. Formation of graphene-nanoparticle can boost its performance for many advanced sensing applications. The characteristics of the nanohybrids are dependent on the nanoparticle size and shape alongwith method of preparation of graphene.

Graphene possesses an advantage of having wide absorption spectrum owing to its zero band gap. Graphene based optical detectors have ultra-wide optical bandwidth. Graphene exhibits electrical bandwidth ~ 500 GHz, theoretically [1].The photoelectric output of the graphene-based photodetector is highly adjustable and nonlinear due to its optical responsiveness and saturable absorption properties. Hybridizing different semiconductor nanoparticles with graphene may reduce the recombination rate of charge carriers, thereby improving the charge separation efficiency. However, the electrical characteristics of the nanohybrid rely on the type of interactions between graphene and the formed nanoparticles. Hence in this study, a simple methodology has been illustrated in which the nanoparticles are directly grown at the defective/functional sites on graphene sheets. Electrical measurements of the nanohybrid have been recorded in dark and under ultraviolet light. SnO$_2$-rGO nanohybrid combines the graphene attributes alongwith SnO$_2$ nanoparticles thereby acting as an excellent material for optoelectronic applications.

2. Experimental Details

2.1 Synthesis process of GO

Graphene Oxide (GO) was prepared according to the Hummers method involving a little modification of avoiding $NaNO_3$ as a precursor. Fixed weight % of Graphite powder was mixed with concentrated H_2SO_4 (82 mL) and H_3PO_4 (18 mL) while stirring. $KMnO_4$ was gradually poured into graphitic mixture and it was kept on stirrer at room temperature for 72 hours. As soon as the oxidation process completed, 5mL of H_2O_2 was added changing the colour to vivid yellow. Deionized water diluted the solution. Filteration (HCL+DI), washing sonication was done for exfoliating GO sheets. It was then centrifuged at 10,000 rpm and kept to dry under ambient conditions for further storage

2.2 Synthesis of rGO-SnO₂ nanoparticle hybrid

Tin oxide, being n-type semiconductor having a good energy bandgap, has numerous applications like conducting electrodes, transparent coatings, solar cells and gas sensors. Researchers have been able to create improved electronic devices by combining the excellent electrical characteristics of rGO with the conducting abilities of SnO_2. These studies revealed that graphene decoration with SnO_2 nanoparticles is a valuable technique for developing high-performance functional gas sensors and optoelectronic devices [2]. In order to prepare SnO_2-rGO nanohybrid, a definite wt. % of GO dispersion (4.8 mg/mL) was added into 50mL of DI water. 2mL of tin dichloride ($SnCl_2.2H_2O$) was added to 50mL HCl solution (1mL of conc. HCl diluted to 50 mL). The reaction mixture was mixed by magnetic stirring and ultrasonicated for 10 minutes. The final mixture was kept on a stirrer at 100ºC for 5h. The SnO_2-rGO nanoparticles hybrid was cleansed a few times with DI and collected by centrifugation and vacuum dried at 100ºC.

The heterojunction establishment at the interface of rGO and SnO_2 is favourable as it improves the optoelectronic characteristics. Figure 1 displays the energy/band structure of SnO_2-rGO heterojunction. SnO_2 and rGO have bandgap differences of 3.60eV and 0.40eV, respectively [3] and work functions with values 4.50eV and 5.00eV, respectively [4,5]. In SnO_2-rGO hybrid electrons flow from SnO_2 towards rGO while holes travel from rGO to SnO_2 uptill achieving an equilibrium condition, thereby forming a depletion layer at the junction [6].

3. Characterizations

X-ray diffractometry of the sample was observed using Bruker D8 Advance X-ray diffractometer (using Cu Kα with λ=0.154nm). Surface morphology was examined using FESEM (Hitachi SU8010). FTIR (Shimadzu IR affinity1S) spectrometer was employed to investigate functional groups. Shimadzu UV2600 spectrometer was employed to measure UV–Visible spectrum (200-800 nm). Keithley sourcemeter 2461 was used to record the I-V measurements with voltage ranging from -1V to +1V. The Multi Auto Lab-203, Metrohm Electrochemical workstation, was used for all electrochemical measurements.

4. Results & Discussion

4.1 Characterizations of SnO₂-rGO hybrid

In the XRD pattern (figure 2), the formed SnO_2 has been crystallized and all the peaks are attributed to rutile SnO_2 (JCPDS 41-1445).The wide peaks with modest intensities represent the formation of tiny crystalline SnO_2 particles [7]. The major peaks occurring in the XRD pattern of the pure SnO_2 nanocrystals are attributed to (110), (101), (211) and (220) reflections of the tetragonal SnO2 phase (JCPDS card no. 41-1445). The peak locations of the SnO_2-rGO specimen resemble pure tetragonal phase of SnO_2. It should be noticed that following the immobilization of SnO_2 nanoparticles onto rGO nanosheets owing to the interaction among the GO and Sn^{2+} ions, the distinct peak at $2\theta = 10.90°$ vanishes and the peaks corresponding to SnO_2 widen. The widening of the peaks may be related to the lower crystalline size of SnO_2 nanoparticles, which can be determined by using Scherrer equation written as:

$$\tau = K\lambda / \beta Cos\Theta$$

The crystallite size of the as-prepared sample is ~14.23 nm.

The SnO_2 nanoparticles immobilized on the rGO nanosheets are responsible for destroying the long range orderliness through the stacking of SnO_2-rGO blocks, as well as turning of graphene oxide to rGO accounts for the absence of $2\theta = 10.90°$ peak [8].

FESEM (figure 3) was accomplished to learn more about the surface structure of the SnO_2-rGO nanohybrids. These images at different magnifications show the distribution of SnO_2 nanoparticles in between graphene sheets.

The compositional characteristics of the sample specimen have been analyzed by EDS as shown in figure 4. The prominent peaks for Sn, O and C elements ascertain the presence of SnO_2 alongwith graphene in the nanohybrid.

Figure 5 shows the UV-Visible spectra for SnO_2-rGO nanohybrid. The absorption peak around 270 nm accounts for reduced graphene oxide [9]. There is an absorption peak around 300nm, which shows the absorption band for SnO_2. Energy bandgap is determined from Tauc's plot shown in inset, which is found to be 3.56eV.

Figure 6 shows the FTIR spectrum of SnO_2-rGO. Peak appearing at $1640 cm^{-1}$ corresponds to C=C. The band located at $630 cm^{-1}$ spectrum indicates the antisymmetric O–Sn–O stretching vibrations, highlighting the existence of SnO_2 nanoparticles onto the layers of exfoliated GO [10]. .

The Raman scattering results (figure 7) of the nanohybrid displayed essential peaks entitling carbonaceous materials at $~1350 cm^{-1}$ and $~1592 cm^{-1}$ [11]. The disturbance caused by graphite amorphization induces a rise in the intensity ratio I_D/I_G, when the sp^2 domain size decreases. The I_D/I_G ratio for the nanohybrid is 1.04. The greater strength of the D-band than that of the G-band, suggests more flaws and structural disturbances.

Cyclic voltammetry (CV) stands as a pivotal and prevalent electrochemical technique utilized for the examination of oxidation and reduction processes, as well as for probing electron transfer reactions. In this methodology, a potentiostat serves as the apparatus of choice, enabling the measurement of the current response of an electrode in relation to a sample electrode, mostly employing the Ag/AgCl electrode [12].Figure 8(a) presents a set of CV curves depicting the behavior of SnO_2/rGO under varying scan rates from 20 mV/s-100 mV/s. Notably, these CV curves exhibit a nearly rectangular configuration, also featuring anodic and cathodic peaks. It is noteworthy that the least discernible variations are observed at higher scan rates, signifying commendable supercapacitive attributes in the material under investigation. Furthermore, these curves lend support to the dual characteristics of double layer and pseudo-capacitance. Specific capacitance values for SnO_2/rGO were subsequently determined at different scan rates, yielding results of 136.83, 121.45, 110.71, 98.29 and 89.16 F/g starting from 20 with an increment of 20V/s respectively. The observed decline in specific capacitance with increasing scan rate that the primary factor influencing the energy storage process is charge diffusion. At lower scan rates, there exists sufficient time for the electrolyte to pass through the larger electrode's pores, giving rise to a markedly enhanced specific capacitance [13,14].

Electrical Impedance Spectroscopy (EIS) was employed to investigate the supercapacitive electrode (depicted in Figure 8(b)) through a frequency sweep spanning from 0.1 Hz to 100,000 Hz. The Nyquist plot obtained for SnO_2/rGO exhibited a notably compact semi-circular segment with a diminished radius, complemented by a more prominent vertical line. Remarkably, the total internal resistance of the SnO_2/rGO electrode was determined to be a mere 1.25 Ω. This impressively low resistance value is responsible for the performance of the supercapacitor.

4.2 Photocurrent Measurement

UV light occupies the energy area in the electromagnetic spectrum inbetween the X-rays and the visible range. Table 1 shows the different wavelengths of UV lamps used in our study. Figure 9 shows the image of a screen electrode employed for taking I-V calculations.

Table 1: Wavelength separations in UV region.

Name	Abbreviation	Wavelength(nm)	Photon Energy(eV)
Ultraviolet-A	UV-A	~357	~3.52
Ultraviolet-B	UV-B	~297	~4.18
Ultraviolet-C	UV-C	~190	~8.41

The sensitivity (S) and responsivity (R) of the specimens are computed as follows:

$$S = I_{Ph}/I_D \qquad (1) \qquad\qquad R = [I_{Ph}-I_D/P_{op}] \qquad (2)$$

where: I_{Ph} denotes photocurrent; I_D denotes dark current; and P_{op} denotes the optical power of the UV lamp.

Figure 10 (a) depicts the I vs V attributes of the SnO_2-rGO nanohybrid, whereas figure 10 (b) displays its ln(I) vs V plot. The experimental investigations for the sample were observed both in the dark and under the ultraviolet light. The sensitivity was calculated as 4.37 for SnO_2-rGO nanoparticle hybrid and the responsivity value as 0.426μA/W. Figure 11 displays the sensitivity(%) achieved with time for the SnO_2-rGO nanohybrid.

5. CONCLUSION

The prime goal behind this study is to synergise the light sensitive capabilities of nanoparticles alongwith exceptional electrical attributes of graphene. The nanohybrid has given a good response to the UV light incidented upon it. SnO_2, like many photocatalytic semiconductors, can create photogenerated electrons and holes, which alter the properties as well as surface states of GO, rGO or SnO_2 itself when exposed to UV light and display a good photoresponse.

ACKNOWLEDGEMENT

FUNDING DECLRATAION

REFERNCES

1. High-Speed Traveling-Wave Modulator Based on Graphene and Microfiber.
Xu K, Xie Y, Xie H, Liu Y, Yao Y, Du J, He Z, Song Q.
J. Lightwave Technol. (2018), **Vol (36), pg. 4730-4735**.

2. Fast facile synthesis of SnO2/Graphene composite assisted by microwave as anode material for lithium-ion batteries.
Shi S, Deng T, Zhang M, Yang G.
ElectrochimicaActa 246 (2017), pg. 1104–1111

3. Nitrogen dioxide-sensing properties at room temperature of metal oxide-modified graphene composite via one-step hydrothermal method.
Zhang D, Liu J, Xia B.
J. Electron. Mater. (2016), **Vol (45), 4324–4330.**

4. Room temperature hydrogen gas sensor based on palladium decorated tin oxide/molybdenum disulfide ternary hybrid via hydrothermal route.
Zhang D, Sun Y, Jiang C, Zhang Y.
Sens. Actuators B (2017), **Vol (242), pg. 15–24.**

5. Seed/catalyst free growth and self-powered photoresponse of vertically aligned ZnO nanorods on reduced graphene oxide nanosheets.
Yang H, Li J, Yu D, Li L.
Cryst.Growth Des. (2016), **Vol (16), pg. 4831–4838.**

6. Graphene schottky diodes: An experimental review of the rectifying graphene/semiconductor heterojunction.
Di Bartolomeo A.
Phys. Rep. (2016),**Vol (*606*), pg. 1–58.**

7. Biogenically structural and morphological engineering of Trigonella foenum-graecum mediated SnO_2 nanoparticles with enhanced photocatalytic and antimicrobial activities.
Goyal Vikas, Singh Arashdeep, Singh Jagpreet, Kaur Harpreet, Kumar Sanjeev, Rawat, Mohit.
Materials Chemistry and Physics (2022),**Vol (282),pg. 125946.**

8. Normal-pressure microwave rapid synthesis of hierarchical SnO_2@rGO nanostructures with superhigh surface areas as high-quality gas-sensing and electrochemical active materials.
Yin L, Chen D, Cui X,GeL Yang J, Yu L Zhang B Zhang R.
Nanoscale.(2014), **Vol (6), pg. 10.**

9. Nanoscale Perforation of Graphene Oxide During Photoreduction Process in the Argon Atmosphere.
Rabchinskii M, Shnitov V, Dideĭkin A, Aleksenskii A, Vul S, Baidakova, M, Pronin I, Kirilenko D, Brunkov P, Weise J, Molodtsov S.
The Journal of Physical Chemistry C. (2016), **Vol (120).**

10. Synthesis and luminescence properties of SnO_2 nanoparticles.
Gu F, Wang SF, Song CF, Qi YX, Zhou GJ, Xu D, Yuan DR.
ChemPhysLett(2003) , **Vol (372) , pg. 451–454.**

11. One-pot synthesis of carbon coated SnO_2/graphene-sheet nanocomposite with highly reversible lithium storage capability.
J. Cheng, H. Xin, H. Zheng, B. Wang,
Journal of Power Sources 232 (2013), **pg. 152–158.**

12. A practical beginner's guide to cyclic voltammetry.
N. Elgrishi, K.J. Rountree, B.D. McCarthy, E.S. Rountree, T.T. Eisenhart, J.L. Dempsey.
J. Chem. Educ., 95 (2018), **pg. 197-206**.

13. $CuWO_4$: A promising multifunctional electrode material for energy storage as in redox active solid-state asymmetric supercapacitor and an electrocatalyst for energy conversion in methanol electro-oxidation
V. Gajraj, C.R. Mariappan.
 J. Electroanal. Chem., 895 (2021).
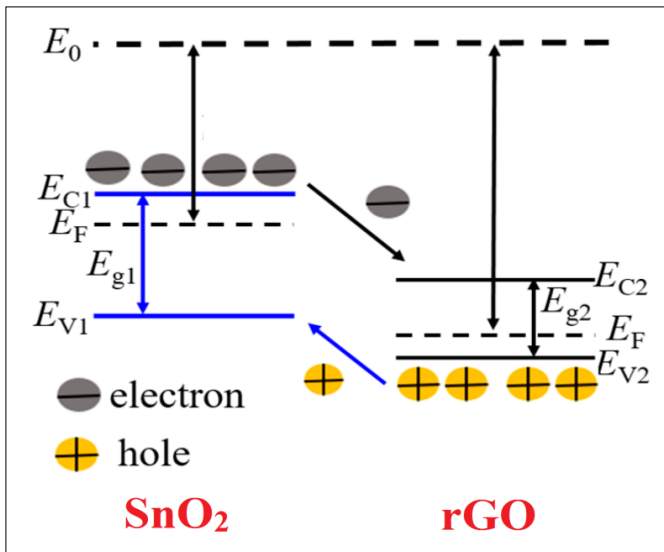
LIST OF FIGURES

Figure 1. Energy-band structure of the SnO$_2$-rGO heterojunction.

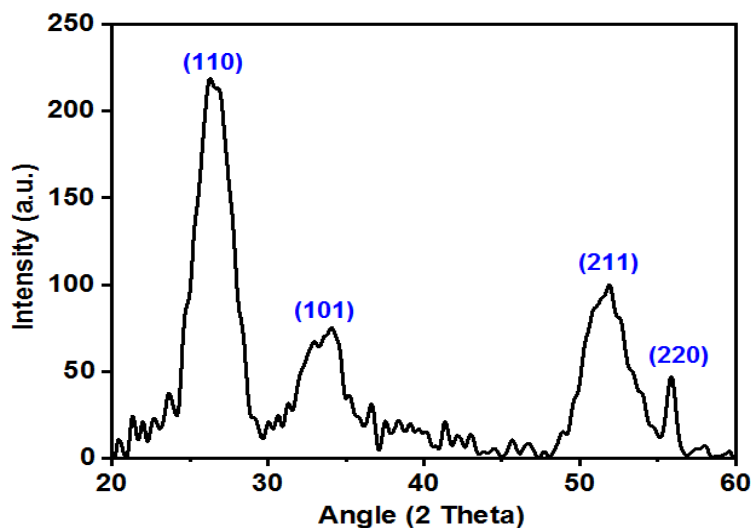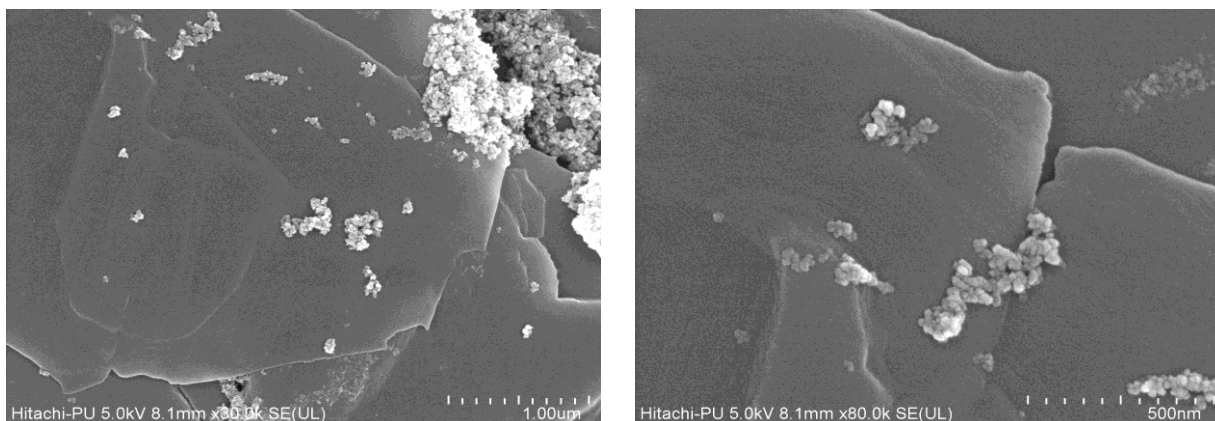**Figure 2. XRD pattern of SnO$_2$-rGO nanoparticle hybrid.**

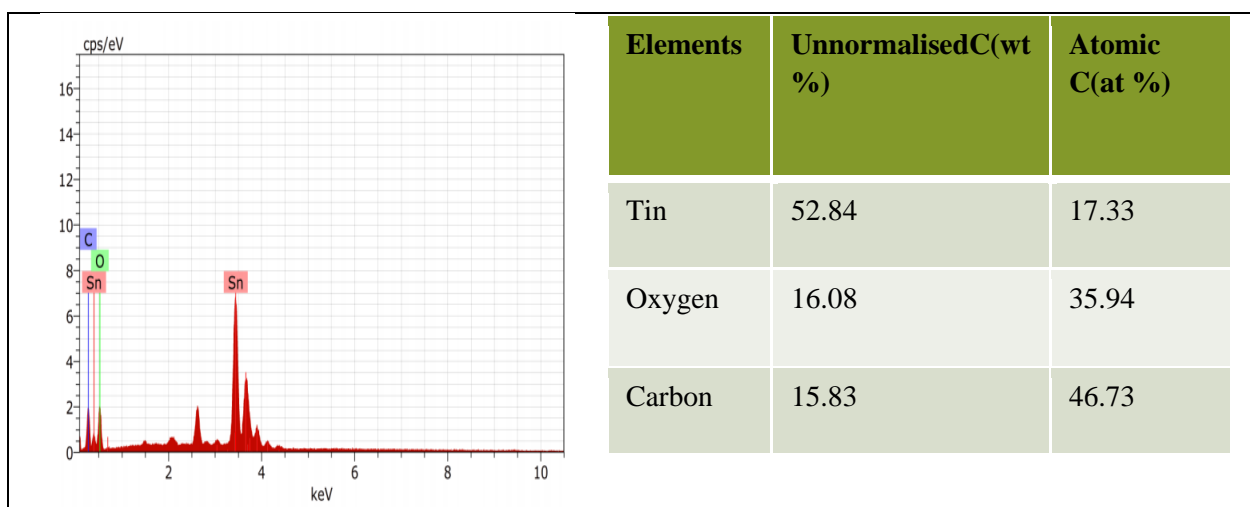**Figure 3. FESEM images of SnO₂-rGO nanohybrid at high magnifications.**

Elements	UnnormalisedC(wt %)	Atomic C(at %)
Tin	52.84	17.33
Oxygen	16.08	35.94
Carbon	15.83	46.73

Figure 4. EDS scan for SnO₂-rGO nanohybrid displaying atomic and wt% of the elements present.
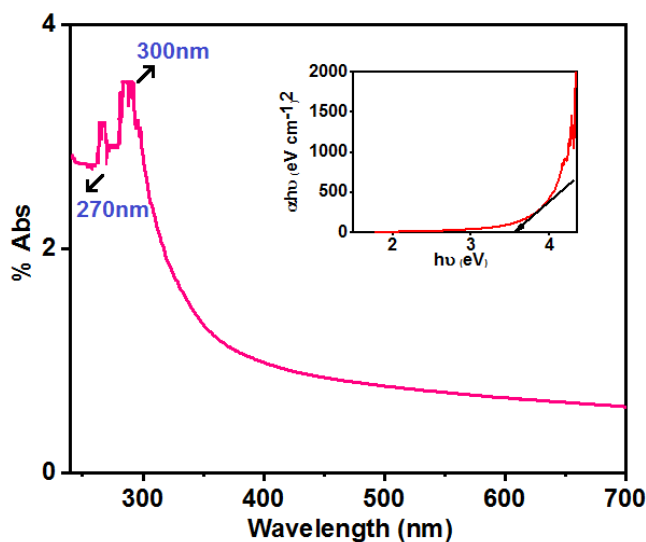
Figure 5. UV-Visible spectrum and tauc plot (inset) of SnO₂-rGO.
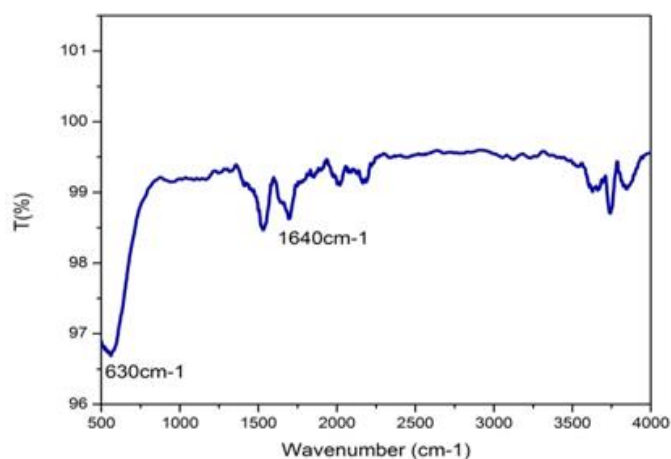
Figure 6. FTIR spectrum of SnO₂-rGO nanohybrid.
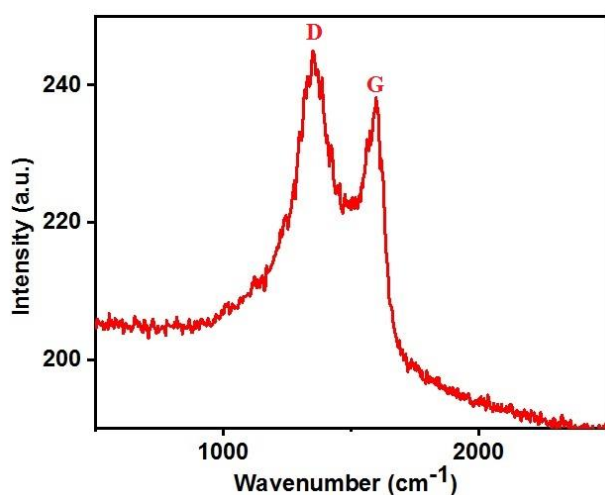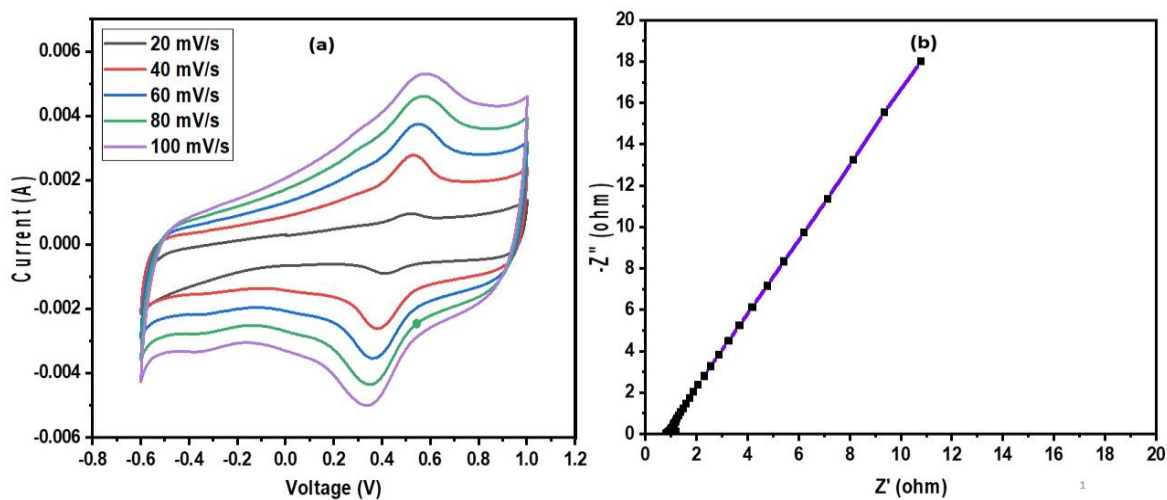

Figure 7. Raman spectrum of SnO₂-rGO nanohybrid.

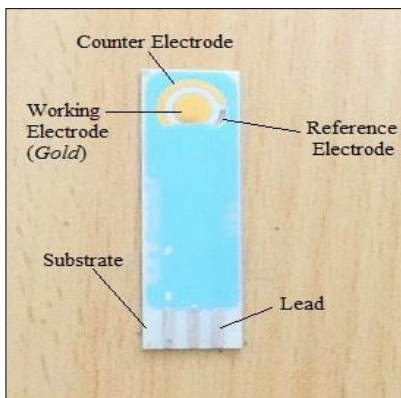**Figure 8. (a) Cyclic Voltammetry of SnO₂/rGO nanocomposite at different scan rate and 8(b) Nyquist plot of SnO₂/rGO**
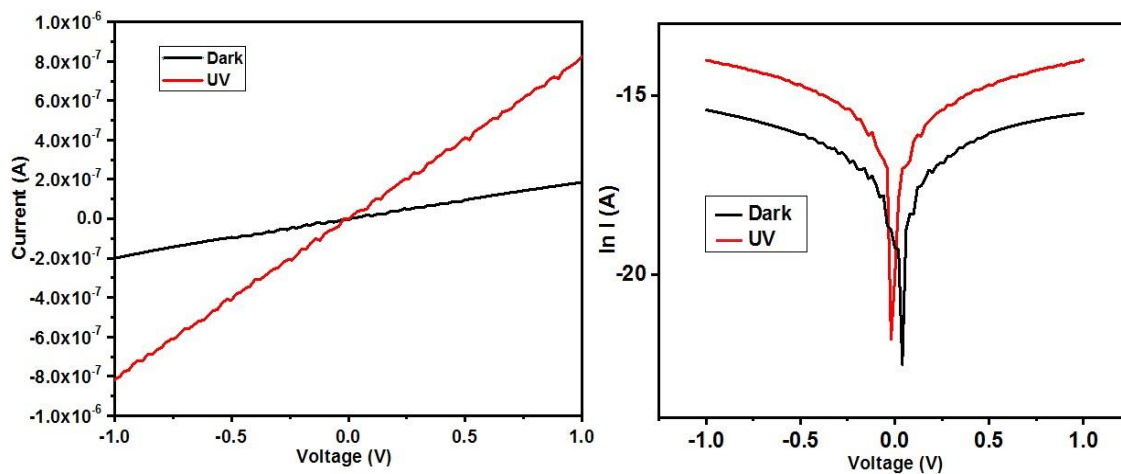

Figure 9. Screen Electrode used for I-V measurements.

Figure 10(a). Current-Voltage (I-V) characteristics and 10(b). ln(I) vs V plot of SnO₂-rGO nanoparticles hybrid in presence and absence of ultraviolet light.
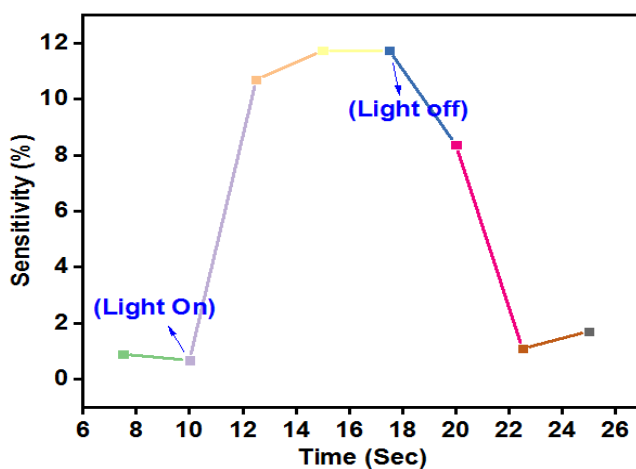

Figure 11. Sensitivity(%) versus time plot of SnO₂-rGO nanohybrid for sensing Ultraviolet light.